

# Practical Condition Monitoring Techniques for Offshore Wind Turbines

J. Xiang, *Member, IEEE*, Simon J. Watson, *Member, IEEE*,  
CREST, Loughborough University, LE11 3TU,UK, s.j.watson@lboro.ac.uk

**Abstract** — Condition monitoring of wind turbines has become important particularly for offshore wind farms. However modern offshore wind turbines are operated at variable speed and the offshore environment is technically challenging, Therefore online condition monitoring and relatively complex data processing methods are crucially needed. This paper presents some new methodologies and results of work to analyze both ten-minute standard SCADA data and medium frequency sampled power data for the purposes of detecting potential faults, particularly in the wind turbine drive train. The SCADA data have been de-trended or daily screened over time. Power data sampled at 30Hz /32Hz have been analyzed using Morlet wavelet transform, Fast Fourier Transform (FFT) and root mean square (RMS). Some examples, including the detection of the potential generator shaft misalignment and generator bearing fault from the slip frequency components in a power signal, are discussed.

**Index Terms**—Morlet wavelet transform, amplitude compensated Morlet wavelet, variable speed, pitch-regulated wind turbine, real-time condition monitoring, electrical power.

## I. INTRODUCTION

Condition monitoring of large wind turbines for offshore is more challenging due to the variable wind loading, variable rotor speed and tough offshore environment. To improve the cost-effective performance of the condition monitoring (CM) offshore, simple and effective technologies should be considered and developed. As there already have some measurements available in wind energy industries, we have reviewed the data availability and developed some practical CM technologies to detect potential faults by using relative simple measurements in wind turbines. Figure 1 gives a summary of the new CM technologies described in this paper.

The main idea of the technologies is to monitor the severity level of a developing fault in wind turbines by comparing the latter to previous calculations.

The technologies in figure 1 have been applied to some standard wind turbine ten-minute SCADA data as well as supplementary 30Hz or 32Hz generator power data from doubly-fed induction generator, variable speed, pitch-regulated wind turbines.

In this paper, the mainly concerned parameters of wind turbines are temperature, acceleration, pitch angle, yaw direction and electrical active power.

Analysis of other SCADA signals from a larger number of wind turbines, including temperature measurements in other locations in the generator and gearbox as well as yaw and pitch measurements is included in this paper.

In order to clearly clarify the multi-background algorithms related to the new technologies, the paper will be organized

as follows: Section II presents the wavelet background; Section III briefly describes the developed state-of-the-art technologies for condition monitoring; Section IV presents the algorithm and demonstrates some results; Conclusions are given in Section V.

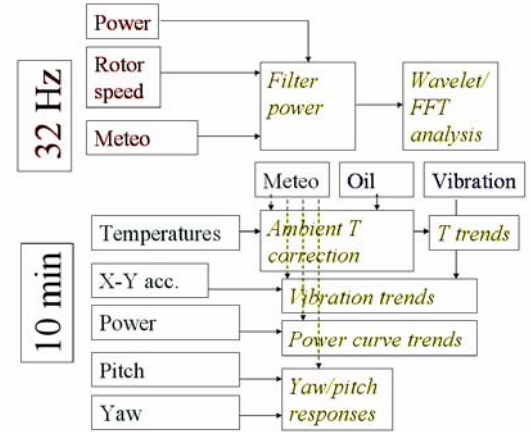


Figure 1. CM technology diagram

## II. WAVELET BACKGROUND

In this paper, the continuous wavelet transform (CWT) is used to extract the individual vibration waveform of each mechanical component, with both frequency and time information, in the electrical power signal of a wind turbine. The discrete Wavelet Transform (DWT) is used as a group of filters to preprocess the electrical power.

### A. The continuous wavelet transform

By definition, the wavelet transform is given in the following relationship<sup>[1]</sup>:

$$W_s(a, b) = \frac{1}{\sqrt{a}} \int_{-\infty}^{\infty} s(t) h^* \left( \frac{t-b}{a} \right) dt \quad (1)$$

$$= \int_{-\infty}^{\infty} s(t) h_{ab}^*(t) dt$$

where  $h(t)$  is generally called the mother wavelet,  $a$  is the scaling parameter and  $b$  is the shift parameter. The shifted and scaled functions  $h_{ab}(t)$  is called the daughter wavelets and given by:

$$h_{ab}(t) = \frac{1}{\sqrt{a}} h \left( \frac{t-b}{a} \right) \quad (2)$$

As wavelet shifts along the time axis, Equation 1 can be rewritten using the variable  $t$  instead of  $b$ , and the variable  $\tau$  instead of  $t$

$$W_s(a, t) = \frac{1}{\sqrt{a}} \int_{-\infty}^{\infty} s(\tau) h^* \left( \frac{\tau - t}{a} \right) d\tau \quad (3)$$

Equation 3 can also be expressed using the correlation operation  $\otimes$  and the convolution operator  $*$

$$W_s(a, t) = s(t) \otimes h_a^*(t) = s(t) * h_a^*(-t) \quad (4)$$

The function  $h_a(t)$  is given by

$$h_a(t) = \frac{1}{\sqrt{a}} h\left(\frac{t}{a}\right) \quad (5)$$

In graphics mode, convolution of two signals involves reversing one of the signals, then shifting it and multiplying by another signal. Correlation only involves shifting it and multiplying (no reversing). Correlation measures the similarity between two signals. Therefore, we can use cross-correlations between multiple wave modes to detect periodic signals at specified frequency. In this concept, for example, the cross-correlations between Morlet wavelet with a specified center frequency and the electrical power of a wind turbine extract the periodic vibration signal of a wind turbine component.

Take Morlet wavelet shown in figure 1 as an example. Morlet mother wavelet has the formula: <sup>[2-3]</sup>

$$h(t) = e^{-t^2/2} \cos(5t) \quad (6)$$

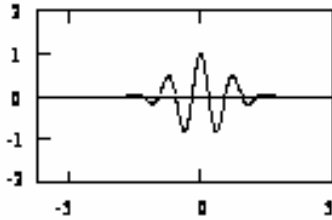


Figure 1: Morlet mother wavelet  $h(t)$

According to equation 2, we have the daughter wavelet

$$h_{ab}(t) = \frac{1}{\sqrt{a}} e^{-\frac{(t-b)^2}{2a}} \cos\left(\frac{5(t-b)}{a}\right) \quad (7)$$

It is obviously that the daughter wavelet is a dilated mother wavelet in time domain when  $a > 1$ ; and a compressed mother wavelet in time domain when  $a < 1$ .

Using Morlet wavelet transform, we can obtain a set of the wavelet coefficients. The set of wavelet coefficients with the highest amplitude is the signal that has the highest similarity to the analyzed signal. The obtained time information includes the signal shape and its broken points, and the frequency information provides the frequency value of the signal. The center frequency of the wavelet coefficients is equal to the frequency value of the analyzed signal.

The principle above will be applied to the electrical power to monitor the mechanical components in wind turbines. If the amplitude of the frequency component of a mechanical component is generally increased under the same operation

condition, a potential fault is properly appearing in the mechanical component.

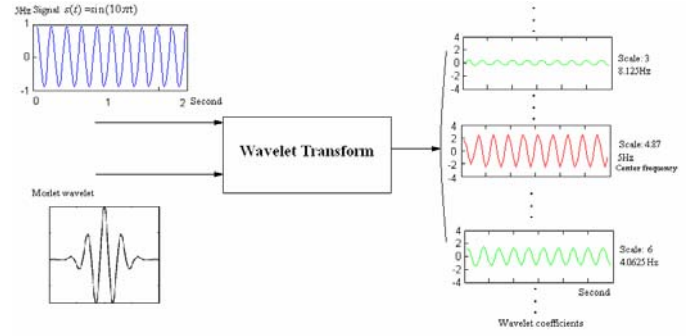


Figure 2 Wavelet coefficients of a single sinusoidal signal

Next, we theoretically explain how to use the wavelet transform to calculate the amplitude of a sinusoidal signal.

According to the convolution theorem that convolving two sequences is the same as multiplying their Fourier transforms, the expression of Equation 4 in angular frequency domain is given by <sup>[4-8]</sup>

$$W_s(a, \omega) = S(\omega) H_a(\omega) \quad (8)$$

where  $W_s(a, \omega)$ ,  $S(\omega)$  and  $H_a(\omega)$  are the Fourier transforms of  $W_s(a, t)$ ,  $s(t)$  and  $h_a(t)$  respectively.

As Morlet wavelet is symmetrical and a band-pass filter with a center frequency, the wavelet coefficients  $W_s(a, \omega)$  has the highest amplitude when the center frequency of the wavelet  $h_a(t)$  is equal to the frequency of the signal  $s(t)$ , say the highest correlation, if  $s(t)$  is a single frequency signal. Figure 2 shows that the wavelet coefficients of a sinusoidal signal has the highest amplitude at the center frequency. If the signal  $s(t)$  is a multi-frequency signal, the wavelet can work out the amplitude of the frequency component at the center frequency of the wavelet.

Figure 3 is the Fourier Transform of Morlet wavelet transform of a single-frequency sinusoidal signal at different frequencies. Figure 3 is calculated from Matlab Wavelet Toolbox. It is obvious that the bandwidth increases with the increase of the center frequency (decrease of the scale) and the amplitude at the center frequency decreases with the increase of the center frequency, even though the amplitude of the signal at all the frequencies is fixed. To solve the problem, next we discuss an amplitude compensated Morlet wavelet.

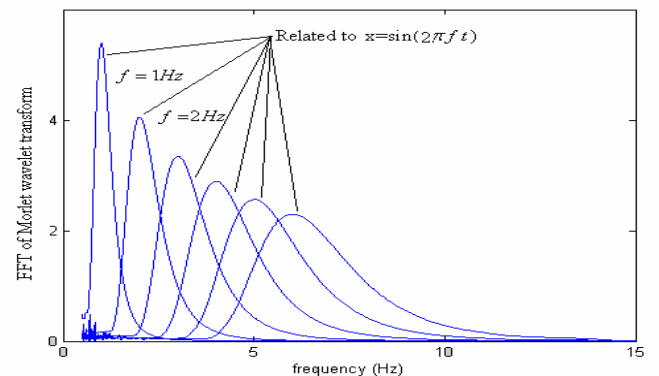


Figure 3 Fourier Transform of Morlet wavelet transform of some single sinusoidal signals

The amplitude compensated Morlet wavelet is to correct the amplitude error of the traditional Morlet wavelet.

Applying the scaling theorem to Equation 5,  $H_a(\omega)$  can be written as

$$H_a(\omega) = \sqrt{a}H(a\omega) \quad (9)$$

where  $H(\omega)$  is the Fourier transforms of  $h(t)$ .

The Fourier Transform of Morlet wavelet in equation (6) is given by

$$H(\omega) = \frac{1}{2}\sqrt{2\pi}(e^{-(\omega-5)^2/2} + e^{-(\omega+5)^2/2}) \quad (10)$$

According to Equation (9), the Fourier Transform of the scaled version Morlet wavelet in equation (5) is thus given by:

$$H_a(\omega) = \sqrt{\frac{\pi a}{2}}(e^{-(a\omega-5)^2/2} + e^{-(a\omega+5)^2/2}) \quad (11)$$

Equation (11) shows that Morlet wavelet in Fourier domain is a band pass filter centered at frequency  $f_{center} = \frac{5}{(2\pi a)}$  with a bandwidth of  $\frac{1}{a}$  Hz.

As  $f = \frac{\omega}{2\pi}$ , we replace angular frequency  $\omega$  with frequency  $f$ . Now the Fourier Transform of Morlet wavelet in frequency domain becomes

$$\begin{aligned} W_s(a, f) &= S(f)H_a(f) \\ &= S(f)\sqrt{\frac{\pi a}{2}}(e^{-(2\pi af-5)^2/2} + e^{-(2\pi af+5)^2/2}) \end{aligned} \quad (12)$$

It can be seen from equation (12) that the frequency components can be estimated from the pick value of the wavelet, if a compensation can be made.

Equation 12 shows that the peak value of  $H_a(f)$  at the center frequency is

$$H_a(f) = \sqrt{\frac{\pi a}{2}}(1 + e^{-(2\pi af+5)^2/2}) \approx \sqrt{\frac{\pi a}{2}} \quad (13)$$

For a sinusoidal function with frequency  $f_0$ , the wavelet transform at the center frequency is

$$\begin{aligned} W_s(a, f)|_{f=f_0} &= S(f)H_a(f)|_{f=f_0} \\ &\approx S(f_0)\sqrt{\frac{\pi a}{2}} \end{aligned} \quad (14)$$

Equation (14) indicates that the amplitude of the signal can be calculated, i.e.  $S(f_0) \approx \frac{W_s(a, f)|_{f=f_0}}{\sqrt{\frac{\pi a}{2}}}$ . Figure 4

and 5 show the wavelet transform of a single-frequency sinusoidal signal at different frequencies before and after compensation calculation. As in Matlab, the Morlet mother wavelet has a constant  $C$ , i.e.  $h(t) = Ce^{-t^2/2} \cos(5t)$ , the amplitude is proportional to the constant  $C$ .

The amplitude in Figure 4 is obtained by using FFT (Fast Fourier Transform) related maximum value estimate. Errors exist when the frequency resolution requirement (0.2Hz in figure 4) is lower than the data length. The error at 2.1, 2.3 and 2.5 Hz is shown in Figure 4. In order to find a precise estimate, we adopt the RSM (Root-Mean-Square) value to estimate the wavelet transform of signals. Figure 5 shows the RMS of Morlet wavelet transform of a sinusoidal signal before and after compensation calculation.

As a conclusion, we can state: Amplitudes of the frequency components in a signal can be estimated from its Morlet wavelet transform. This is especially important for the condition monitoring of wind turbines, where the disturbances caused by faulty turbine elements are non-stationary. The wavelet transform of a non-stationary signal includes the information of the length, the frequency values and the amplitude values of the disturbances. As faults get more serious, the amplitudes of the disturbances become higher. Using Morlet wavelet transform to monitor the amplitudes of the frequency components of turbine elements can allow an on-line automatic operation, which is vital to offshore wind turbines.

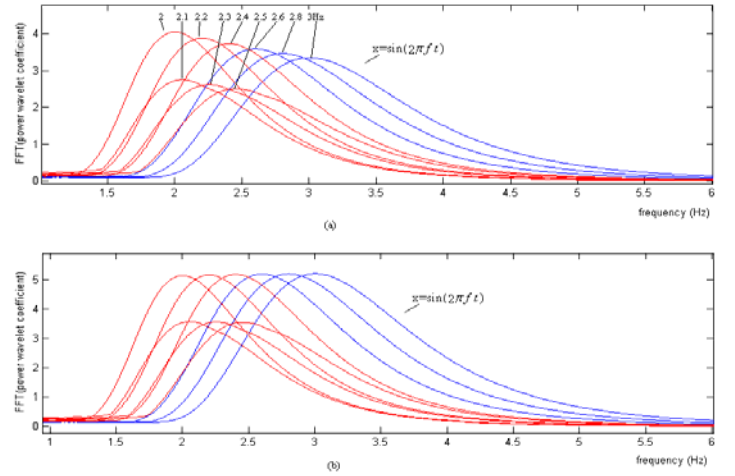


Figure 4 FFT of Morlet wavelet transform of a sinusoidal signal before (a) and after (b) compensation calculation

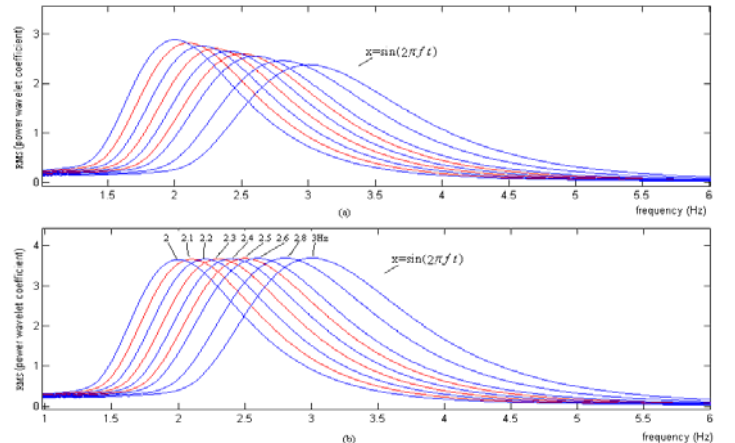


Figure 5 RMS of Morlet wavelet transform of a sinusoidal signal before (a) and after (b) compensation calculation

## B. The discrete wavelet transform (DWT)

Some signals, e.g. the power signal in this paper, have a high constant and are rich of very low frequency components. These frequency components might make some monitored low frequency components unseen in the signal's spectrum. Also window-leakage errors<sup>[9]</sup> affect the calculation precision. Therefore we need a filter to eliminate the high constant component and attenuate the very low frequency components. As Discrete Wavelet Transform (DWT) can be used as a multirate filter that provides computational efficiencies, we will use the discrete wavelet transform to select a subset of coefficients for special analysis.

The Discrete Wavelet Transform is expressed as

$$W_s(j, k) = \int_{-\infty}^{\infty} s(t)\psi_{j,k}(t)dt \quad (15)$$

where  $\psi_{j,k}(t)$  is the discrete expression of the daughter wavelet of Equation 2.

Defining the sampling of the wavelet transform as

$$a = a_0^j, \quad b = kb_0a_0^j, \quad j, k \in Z \quad (16)$$

with  $a_0 \neq 1, \quad b_0 \neq 0$

We have the discrete daughter wavelet

$$\begin{aligned} \psi_{j,k}(t) &= \psi_{ab}(a, b) \Big|_{a=a_0^j, b=kb_0a_0^j} \\ &= \frac{1}{\sqrt{a_0^j}} \psi\left(\frac{t - kb_0a_0^j}{a_0^j}\right) \end{aligned} \quad (17)$$

If we take the dyadic sampling ( $a_0 = 2, b_0 = 1$ ) to the daughter wavelet, we have

$$\psi_{j,k}(t) = \frac{1}{\sqrt{2^j}} \psi\left(\frac{t - k2^j}{2^j}\right) \quad (18)$$

Where  $j$  is the number of levels in the discrete wavelet transform.

It can be seen that the wavelet is doubly dilated in time domain each time the level  $j$  is increase by 1, which means a half bandwidth. Figure 6 shows the mother wavelet and daughter wavelet in both time and frequency domain for different values of scale with the dyadic sampling.

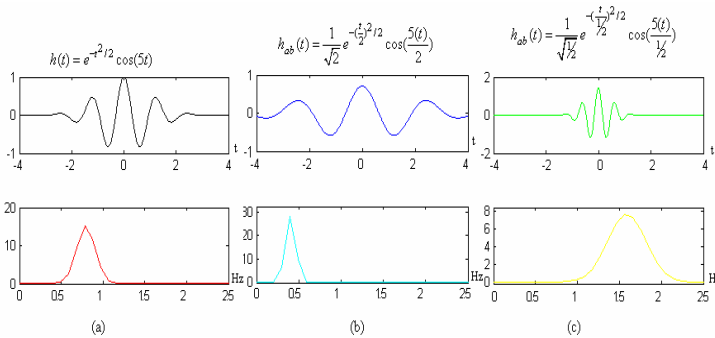


Figure 6. Wavelet for different values of scale with dyadic sampling (a) Mother wavelet (b) Daughter wavelet  $a = 2$

(c) Daughter wavelet  $a = \frac{1}{2}$

Figure 6 implies that DWT provides sets of filters. The bandwidth at  $a = \frac{1}{2}$  is doubled than the bandwidth at  $a = 1$  ;

and the bandwidth at  $a = 2$  is half of the bandwidth at the mother wavelet. It is obviously that more harmonics of a signal are included in the signal's wavelet transform, if the scale gets smaller. With different scales, we can obtain a group of signals that have different amount of harmonics. This means that DWT can be considered as sets of filters that divide a signal frequency band into subbands. If we divide the discrete wavelet transform  $W_s(j, k)$  into two parts: the high-scale (or low-frequency) components of the signal  $s(t)$  and the low-scale (or high-frequency) components of the signal  $s(t)$ . The former is called the approximation coefficients and the latter is called the detail coefficients.

The approximation coefficients of the discrete wavelet transform for the digital signal  $s(k)$  at level  $j$  is<sup>[10]</sup>

$$A_j = \sum_{n=0}^{\infty} s(n)\phi_{j,k}(n) = \sum_{n=0}^{\infty} s(n) \frac{1}{\sqrt{2^j}} \phi\left(\frac{n - k2^j}{2^j}\right) \quad (19)$$

where  $\phi_{j,k}(n)$  is the scaling function associate with the wavelet function  $\psi_{j,k}(n)$ .

The detail coefficients of the discrete wavelet transform for the digital signal  $s(k)$  at level  $j$  is

$$D_j = \sum_{n=0}^{\infty} s(n)\psi_{j,k}(n) = \sum_{n=0}^{\infty} s(n) \frac{1}{\sqrt{2^j}} \psi\left(\frac{n - k2^j}{2^j}\right) \quad (20)$$

From the filter point of view, we can say that the discrete approximation in equation (19) is a low-pass filtering of the signal  $s(t)$  and the discrete detail in equation (20) is a high-pass filtering of the signal  $s(t)$ .

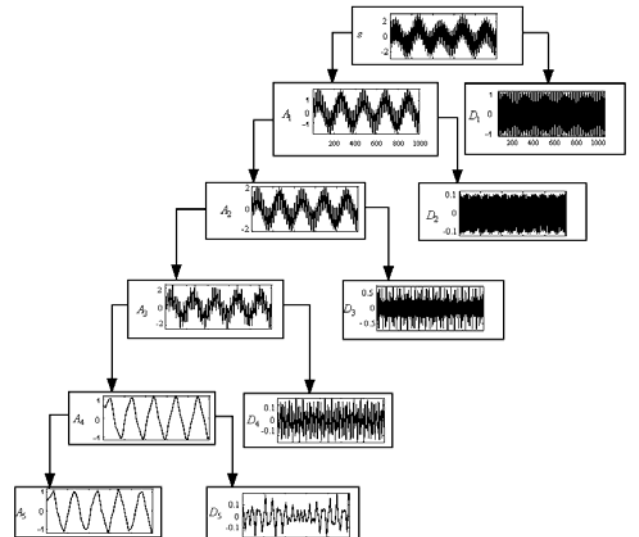


Figure 7 five-stage discrete wavelet transform of a signal

For further understanding of the advantage of the discrete wavelet transform, we give Figure 7 that shows a five-stage discrete wavelet transform of a signal taken from the Matlab Wavelet Toolbox. The low frequency signal 'A4' is extracted from an original signal 's' at the decomposition level 4. Higher frequency signals (details), e.g. 'D', at different decomposition levels are also available from the discrete wavelet transform.

### III. THE DEVELOPED STATE-OF-THE-ART ON CONDITION MONITORING

As the paper aims at the condition monitoring of large offshore variable-speed wind turbines, in which the measurement can't be controlled, we will explain how the measured power data can be used to analyze the vibration frequency components. As to the ten-minute SCADA data, we will discuss the relationship between the turbine component temperature and the electrical power, and the analysis method of pitch and yaw systems.

#### 1. Extracting frequency components of vibration signals from electrical power

The vibration caused by unbalanced wind turbine rotors, shaft, bearing, gearbox and etc can be calculated from electrical power signal in wind turbines<sup>[11-27]</sup>.

##### A. Stator electrical power in steady-state at fix speed

Now we discuss the relationship between the power and the torque in induction machines. It will be revealed that the torques caused by the slip pulsation, the faulty gearbox and blades are included in the electrical power of wind turbines.

The mechanical power and the stator electric power output are computed as follows:

$$P_m = T_m \omega_r \quad (21)$$

$$P_s = T_{em} \omega_s \quad (22)$$

where

$P_m$ : Mechanical power captured by the wind turbine and transmitted to the rotor

$P_s$ : Stator electrical power output

$T_m$ : Mechanical torque applied to rotor

$T_{em}$ : Electromagnetic torque applied to the rotor by the generator

$\omega_r$ : Angular rotational speed of the generator rotor

$\omega_s$ : Synchronous angular speed

For a loss less generator the mechanical equation is:

$$J \frac{d\omega_r}{dt} = T_m - T_{em} \quad (23)$$

where

$J$ : Combined rotor and wind turbine inertia coefficient

In steady-state at fixed speed for a lossless generator  $T_m = T_{em}$  and  $P_m = P_s + P_r$ , where  $P_r$  is the rotor electrical power output.

From eqn. (22), we have

$$P_s = T_{em} \omega_s = T_m \omega_s \quad (24)$$

It follows that:

$$\begin{aligned} P_r &= P_m - P_s \\ &= T_m \omega_r - T_{em} \omega_s \\ &= -T_m \left( \frac{\omega_s - \omega_r}{\omega_s} \right) \omega_s \\ &= -s T_m \omega_s \\ &= -s P_s \end{aligned} \quad (25)$$

Eqn. (24) indicates that the torque is proportional to the stator electrical power output, if the rotor speed is fixed.

Although the wind speed is not controllable, the rotor speed is controlled at some range of wind speed in variable-speed wind turbines. In very low winds, the turbine is operated at nominally constant speed. Figure 8 is a 25-minute power data and generator rotor speed data measured from a large wind turbine. The maximum relative variation of generator rotor speed is less than  $\pm 0.2\%$ . If we ignore the tiny variation, according eqn. (24), the torque frequency components on the generator rotor, including the pulsating torque and vibration torques caused by bearing, gearbox, blades and other turbine elements, will be included in the stator electrical power output.

In fact, the effects of a tiny variation of rotor speed on the stator electrical power output is very small. This can be explained as below.

Donating  $\omega_r$  as the fixed generator rotor and  $\Delta\omega_r$  the variation in the generator rotor, we have

$$P_m = T_m (\omega_r + \Delta\omega_r) \quad (26)$$

$$P_s = T_{em} \omega_s \quad (27)$$

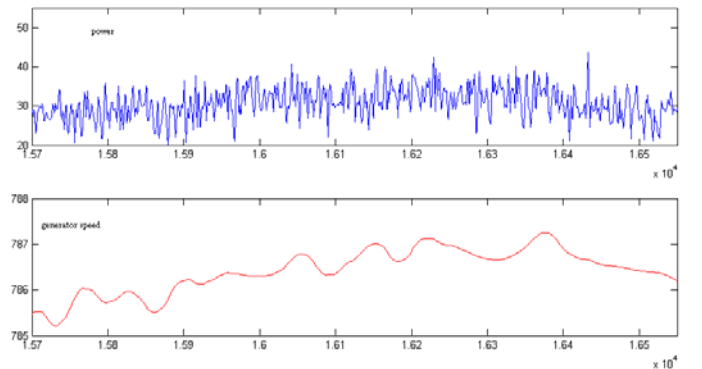


Figure 8 Power and generator speed at low wind speed

According to equation 23, for a lossless generator the mechanical equation is:

$$J \frac{d(\omega_r + \Delta\omega_r)}{dt} = J \left\{ \frac{d\omega_r}{dt} + \frac{d(\Delta\omega_r)}{dt} \right\} \quad (28)$$

$$= T_m - T_{em}$$

It follows that:

$$T_{em} = T_m - J \frac{d(\Delta\omega_r)}{dt} \quad (29)$$

If  $\Delta\omega_r$  is very slow signal, we have  $T_m \approx T_{em}$  and

$$P_s \approx T_m \omega_s \quad (30)$$

### B. Pulsating Torque

It is known that in a symmetrical three-phase machine, if an asymmetrical rotor is presented, there will be unbalanced rotor currents flow in the rotor windings. In the steady-state, the pulsating torque caused by the asymmetrical rotor can be written as

$$T_p(t) = -\left[ \frac{3P}{(2s\omega_s)} \right] \text{Re} \{ [(\bar{U}_{r1}\bar{I}_{r2} - \bar{U}_{r2}\bar{I}_{r1})] e^{j2s\omega_s t} \} \quad (31)$$

In eqn (31),  $\bar{I}_{r1}, \bar{I}_{r2}$  are the positive- and negative-sequence phasor symmetrical components of the rotor current in the steady-state.  $\bar{U}_{r1}, \bar{U}_{r2}$  are the positive- and negative-sequence phasor symmetrical components of the rotor voltages respectively. Eqn (31) shows that the

pulsating frequency component  $2sf_s$ , where  $f_s = \frac{\omega_s}{2\pi}$ , is produced when the rotor of an induction machine is asymmetrical.

### C. Blade-passing frequency

It is known that aero-dynamical asymmetry, e.g. unbalanced angle of attack on blades, can cause a 1p oscillation. Monitoring the amplitude of this 1p oscillation can determine the level of severity of the asymmetry.

If the thrust and the propulsion forces are equal on each blade of the symmetrical rotor, there will be a 3p-frequency torsional oscillation that is three times the turbine rotor angular frequency  $\omega_n$ .

## 2. Monitoring of variation in temperature, pitch angle and yaw direction using standard wind turbine ten-minute SCADA data

Research reveals that there are statistical characteristics of the variation that can be used for condition monitoring of the mechanical components in wind turbines. Next we discuss the characteristics of temperature, yaw direction and pitch angle.

### A. The relationship between component temperature and the electrical power in a wind turbine

It is evident that the temperature of the generator bearing is a nonlinear function of electrical power in figure 8. The large scatters are probably related to anomalies. Figure 9 indicates the temperature to the electrical power lag exists in wind turbines. Therefore we developed some data processing

methods, including detrending and daily screen.

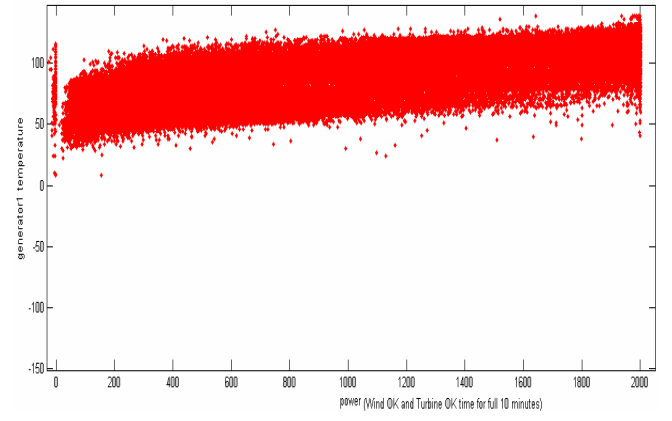


Figure 8 Generator bearing temperature

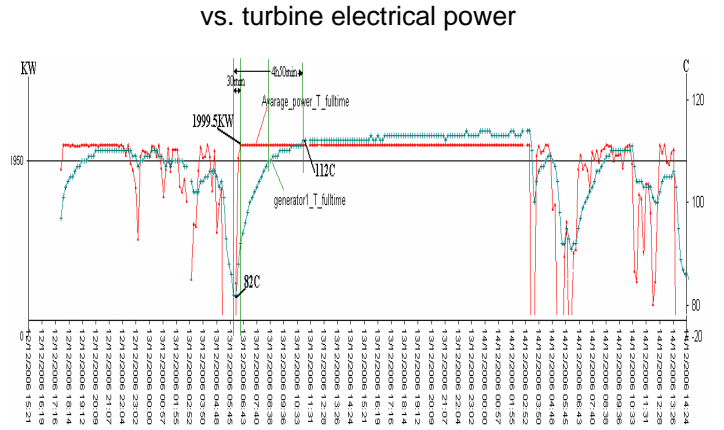


Figure 9. Generator bearing temperature

Lags behind turbine electrical power

### B. Mechanism of controlled pitch angle and yaw direction

In the link motion of the Z-axis, the yaw direction follows the wind direction. Large scatters away from the zero degree are probably related to anomalies.

On a pitch controlled wind turbine, the angle of the blades is actively adjusted by a machine control system. The angle versus the wind speed, for wind speeds above normal, is approximately linear relations. Therefore large scatters away from the trend line are probably related to anomalies.

The detrended pitch angle  $P_{det ren}$  can be

$$P_{det ren} = P_m - P_{fit} \quad (32)$$

$P_m$ : Measured 10-minute average pitch angle

$P_{fit}$ : Fitting curve from measured wind speed and pitch angle

## IV. ALGORITHM AND RESULTS

In this section, we first describe the developed technologies and then demonstrate some results.

For the analysis of standard wind turbine ten-minute SCADA data, the data have firstly been corrected for the effect of ambient temperature changes and considered as a function of power afterwards. In order to detect potential fault modes, the

SCADA data are either de-trended or daily screened in consecutive time units. These data have then been compared with generator power output during a 'training' period of a few months and the resulting trend as a function of power subtracted from subsequent values in the method of detrending. The method of daily screen is to calculate daily maximum variations under the condition that the concerned parameter, e.g. bearing temperature, is nearly a constant regarding to the electrical power in a wind turbine.

For the analysis of 30Hz of 32Hz electrical active power data, the torque frequency components of different mechanical assemblies in the generator power signal are monitored by calculating the magnitudes at the centre frequency or the root mean square (RMS) of their Morlet wavelet coefficients. Figure 10 is an algorithm diagram using the wavelet transform and RMS method. A screen wind is needed as a pre-processor to ensure a nearly constant generator speed and low power that acts as a low noise background regarding to the signal from a faulty mechanical component.

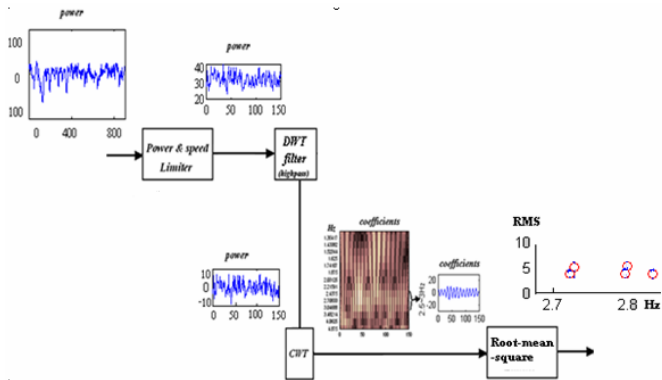


Figure 10 Algorithm diagram

To illustrate the effectiveness of the developed technologies, an application of detecting generator shaft misalignment and bearing failure in two types of large turbines is presented in figure 11 to 13. Results show that the daily screened acceleration, temperature and the power wavelet reflect the effects of the faults. For comparison, other related information and the results from Pruftechnik is also included in figure 12. Figure 14 is an application of the detrending method to 10-minute yaw direction data of a wind turbine in the UK.

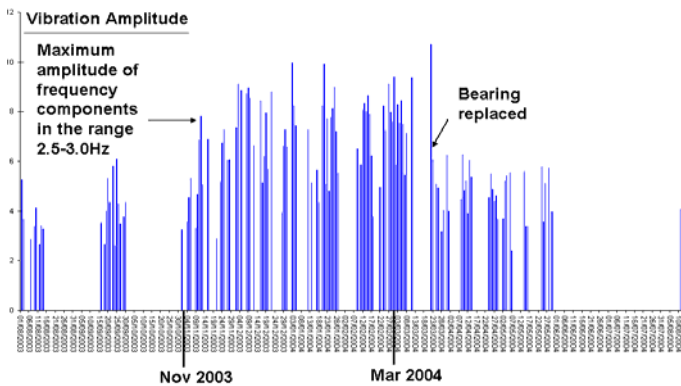


Figure 11: Maximum daily amplitude of the Fourier transformed wavelet filtered GE 1.5S wind turbine power output within the frequency range 2.5 and 3.0Hz.

For GE turbine in figure 11, a 5-second data window is selected with the following limits: Rotor speed: 12~12.5 rpm and Active Power: 20~40Kw. The slip frequency 2.167~3.7 Hz is calculated from operator's information.

For Nordex turbine in figure 12, a 5-second data window is selected with the following limits: Generator speed: 785 ~ 795rpm and active power: 0~55Kw. The slip frequency is  $2sf_s = 2[(1000 - 785)/1000] \times 1000/60 = 6.83 \sim 7.17$  Hz.

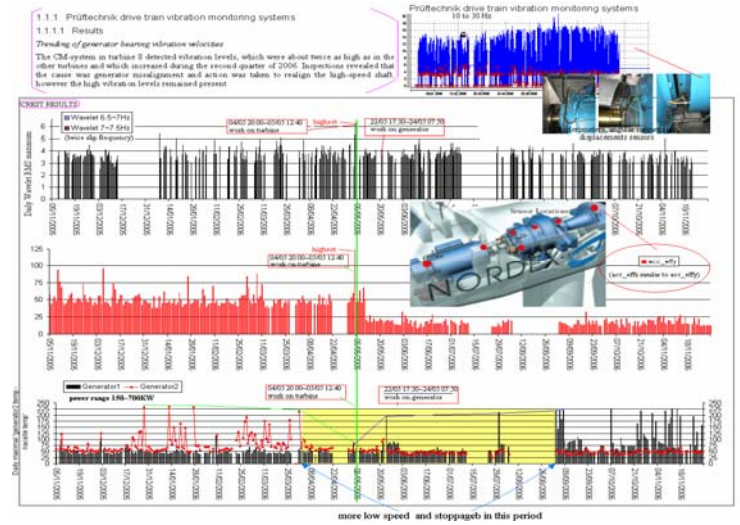


Figure 12 : Maximum daily RMS of one of the wavelet filtered Nordex N80 wind turbine power outputs within the frequency range 6.5 ~7.5Hz, comparing to the vibration, acceleration and temperature results.

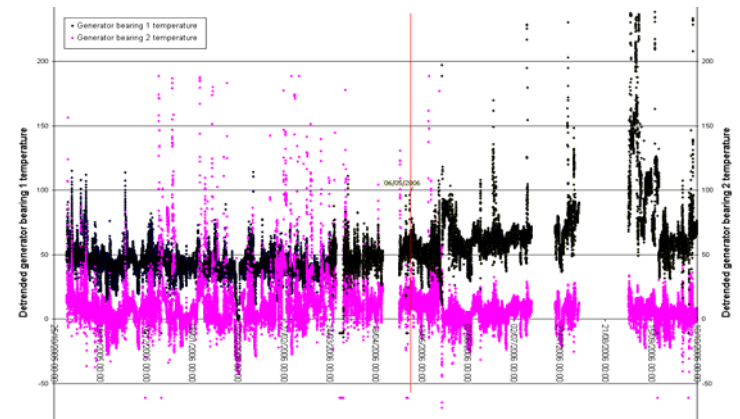


Figure 13 Detrended generator bearing temperature in Nordex N80 wind turbine

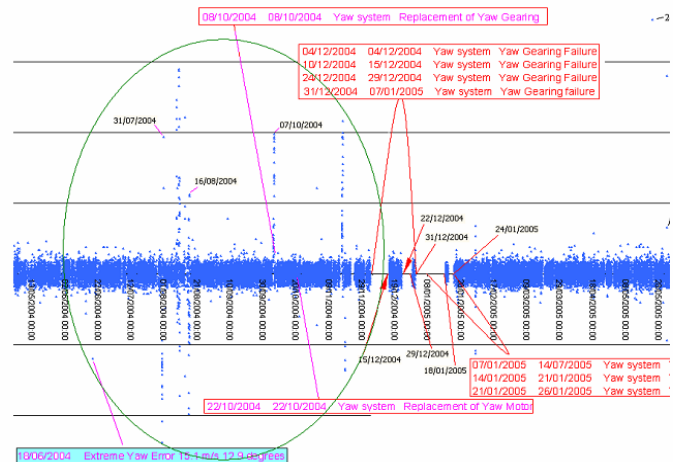


Figure 14. Detrended wind turbine yaw direction

Figure 11 ~12 indicate that the vibration caused by generator misalignment , bearing and other problems can be detected by its related frequency components in the generator power and can be used as an indication of a potential failure in a wind turbine. Figure 13 reveals that 10-minute acceleration,

temperature and yaw direction analysis can provide an online diagnosis of faulty components in a wind turbine.

The results from figure 11 to 14 are automatically calculated using the developed state-of-the-art in Section II. Computer programs are designed to meet the needs of automatic data operation, data preprocessing, signal processing, demonstration and storage of processed data, and etc.

## V. CONCLUSION

This paper has presented some new methodologies and the results of research work to analyze standard wind turbine ten-minute SCADA data as well as supplementary 30Hz/32Hz generator power data. The results show evidence that these technologies are practical, effective and applicable to the online automatic condition monitoring of offshore wind turbines. The wavelet transform related methodology can be simply applied to electrical power to monitor the vibration level caused by misalignment, bearing and other problems. It can be used as a general sign or indication of an unhealthy wind turbine, especially the time length of the change from normal function to a serious malfunction. The trending and daily screen methods for ten-minute SCADA data are useful for an on-line diagnosis to locate fault wind turbine components.

## ACKNOWLEDGEMENTS

The authors would like to thank UK EPSRC, ECN and European industrial partners in the CONMOW project for their ongoing support of this project.

## VI. REFERENCE

- [1] Agostino Abbate, Casimer M. DeCusatis, Pank. *Wavelets and subbands: fundamentals and applications*; Boston : Birkhauser, 2001.
- [2] Yingen Xiong, Francis Quek. Gestural Hand Motion Oscillation and Symmetries for Multimodal Discourse: Detection and Analysis; *cvprw*, 2003; 5: 58.
- [3] Wavelet Toolbox User's Guide, Mathworks.
- [4] N.D et a. Using Time-Frequency and Wavelet Analysis to Assess Turbulence/Rotor Interactions. *Proc. of ASME/AIAA Wind Energy Symp* 2000; 130–149.
- [5] Shyu H-C.; Sun Y-S. *Construction of a Morlet Wavelet Power Spectrum. Multidimensional Systems and Signal Processing*; Springer: Netherlands 2002; 13; 101-111.
- [6] W.J.Phillips: Wavelets and Filter Banks Course Notes,1993;  
<http://www.engmath.dal.ca/courses/engm6610/notes/notes.html>
- [7] Ersoy, Okan K. *Fourier-related transforms, fast algorithms and applications, Upper Saddle River. N.J.:* Prentice Hall, 1997.
- [8] H. Szu, Y. Sheng, and J. Chen. Wavelet transform as a bank of matched filters. *Appl. Opt* 1992; 31:17: 3267-3277.
- [9] Douglas L. Jones I and Thomas. Time- frequency window. leakage in the short-time. fourier transform. *Circuits systems and signal process* 1987; 6:3.
- [10] Lee B.Y.; Tarnng Y.S.1. Drill fracture detection by the discrete wavelet transform. *Journal of Materials Processing Technology* 2000; 99(1:3): 250-254.
- [11] Vas, Peter. *Parameter estimation, condition monitoring, and diagnosis of electrical machines*; Oxford: Clarendon Press, 1993.
- [12] Mathwork, *Wind Turbine Doubly-Fed Induction Generator* (Phasor Type).
- [13] Yang, S. J. *Low-noise electrical motors*; Oxford : Clarendon Press, 1981
- [14] Ahmed Y. Ben Sasi, Fengshou Gu, Yuhua Li, Andrew D. Ball. A validated model for the prediction of rotor bar failure in squirrel-cage motors using instantaneous angular speed. *Mechanical Systems and Signal Processing* 2006; 20: 1572–1589.
- [15] Ahmed Yousef Ben Sasi, Fengshou Gu, Bradley Payne, Andrew Ball. Instantaneous angular speed monitoring of electric motors. *Journal of Quality in Maintenance Engineering* 2004; 10 ( 2 ): 123-135.
- [16] Thiringer, T. Dahlberg, J.-A. Periodic pulsations from a three-bladed wind turbine. *IEEE Transaction on Energy Conversion* 2001; 16(2): 128-133.
- [17] Charles E. Wilson and Peter J Sadle, *Kinematics and Dynamics of Machinery*, Prentice Hall, 2003
- [18] Peter Caselitz. Rotor Condition Monitoring for Improved Operational Safety of Offshore Wind Energy Converters Jochen Giebhardt. *Journal of Solar Energy Engineering* 2005; 127(2): 253-261.
- [19] Morten H. Hansen, Anca Hansen, Torben J. Larsen, Stig Øye, Poul Sørensen and Peter Fuglsang, *Control design for a pitch-regulated, variable speed wind turbine*; Risø National Laboratory, 2005, 1:84.
- [20] Nandi, S. Toliyat, H.A. Xiaodong Li. Condition monitoring and fault diagnosis of electrical motors-a review. *IEEE Transactions on Energy Conversion* 2005; 16( 4): 719- 729.
- [21] Tavner, P, J and Penman, J. *Condition monitoring of Electrical machines*; Research Studies Press: Letchworth, UK., 1987.
- [22] A. Siddique, G. S. Yadava, and B. Singh. A review of stator fault monitoring techniques of induction motors. *IEEE Transactions on Energy Conversion* 2005; 20: 106-114.
- [23] T. Thiringer and J.-A Dahlberg. Periodic pulsations from a three-bladed wind turbine. *IEEE Transactions on Energy Conversion* 2001; 16: 128-133.
- [24] Chin-shun Tsai Cheng-Tao Hsieh Shyh-Jier Huang. Enhancement of damage-detection of wind turbine blades via CWT-based approaches. *IEEE Transactions on Energy Conversion* 2006; 21( 3): 776- 781.
- [25] Shyh-Jier Huang Cheng-Tao Hsieh. High-impedance fault detection utilizing a Morlet wavelet transform approach. *IEEE Transactions on Power Delivery* 1999; 14(4): 1401- 1407.
- [26] Jing Lin, Ming J Zuo, Ken R Fyfe. Mechanical fault detection based on the wavelet de-noising technique. *Journal of vibration and acoustics* 2004; 126:11, 9-16.
- [27] Lin, J., and Qu, L. Feature Extraction Based on Morlet Wavelet and Its Application for Mechanical Fault Diagnosis. *J. Sound Vib* 2000; 234(1):135–148